Chapter 2 – Experimental Methods

2.1 – Detection Methods

A chemical reaction can be studied through monitoring the reactants, intermediates, products, or some combination thereof, depending on the nature of the reaction and the method involved. Consequently, many different techniques have been developed, particularly for studying reactive molecules with short lifetimes and low abundances. There are generally tradeoffs in different techniques, involving a combination of the method's time resolution, sensitivity, spectral resolution, and the ability to identify different molecules.

The work presented in this thesis uses two main techniques, cavity ringdown spectroscopy (CRDS) and laser-induced fluorescence (LIF), to study the reactants and products of chemical reactions.

2.1a – Cavity Ringdown Spectroscopy

For light passing through a chemical sample, the amount of light absorbed is governed by the Beer-Lambert law, which states

$$\ln\left(\frac{I_0}{I_t}\right) = \sigma(\lambda)LN \qquad \text{(Equation 2.1)}$$

where I_0 is the initial intensity of the light, I_t is the intensity of the transmitted light after passing through the sample, σ is the cross section(s) of the sample at wavelength λ (with units of cm^2), L is the pathlength of the sample (units of cm), and N is the number density of the sample (units of cm^{-3}).

For the detection of species that have low concentrations, such as reactive radicals or products of their reactions, Equation 2.1 indicates that the trace molecule must either have a large cross section or be contained in a long chamber. The former is an inherent

property of the molecule, which therefore can not be altered experimentally. One method to the increase the sample length is through cavity ringdown spectroscopy, which can produce pathlengths on the order of kilometers or more. This technique, originally developed in the 1980s, was originally based on methods to precisely and accurately measure the reflectivity of highly reflective mirrors (R > 0.9995)[1] and was first used to measure doubly forbidden electronic transitions of O_2 to demonstrate its sensitivity.[2]

CRDS has been reviewed extensively in the past.[3-4] These measurements rely on two highly reflective mirrors, often plano-concave, attached to the ends of a cell with distance *L*, as seen in Figure 2.1, to form an optical cavity. Light is transmitted into the cavity, bouncing back and forth between the two mirrors. As light hits each mirror, a small portion (1 – R) of the light leaks out and hits a detector. The resulting exponential decay is known as a ringdown. The intensity of the light at time *t,* $i(t)$, in an empty cavity with no absorption of the light, is governed by

$$i(t) = i_0 e^{-(1-R)\frac{tc}{L}} \qquad \text{(Equation 2.2)}$$

where i_0 is the initial intensity of the ringdown, *L* is the distance between the two mirrors, and *c* is the speed of light. The ringdown time, τ, is characterized by the time the ringdown takes to reach $i_0 e^{-1}$, which can be determined by Equation 2.1 to be

$$\tau = \frac{L}{c(1-R)} \qquad \text{(Equation 2.3)}$$

When a molecular absorber is present, the intensity at time *t* instead becomes

$$i(t) = i_0 e^{-\frac{tc}{L}[(1-R)+\sum \alpha_i L]} \qquad \text{(Equation 2.4)}$$

where α_i is the absorption coefficient of species *i* and is defined as

$$\alpha_i = \sigma_i N_i \qquad \text{(Equation 2.5)}$$

With the presence of molecular absorbers, the ringdown time therefore decreases, as the signal decays quicker than without an absorber. The ringdown time then becomes

$$\tau = \frac{L}{c[(1-R)+\sum \alpha_i L]} \qquad \text{(Equation 2.6)}$$

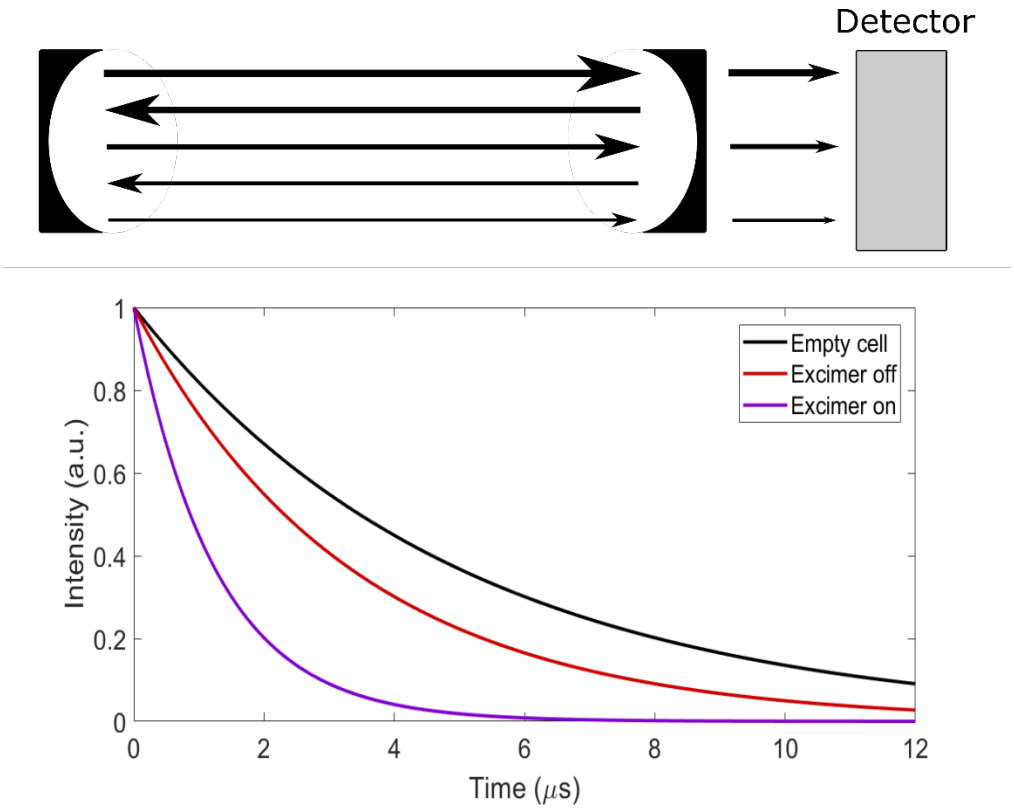

Figure 2.1: Diagram of a cavity ringdown cell (top), showing the light inside the cavity decreasing as it bounces back and forth, and simulated ringdown decays (bottom) of an empty cell (black), with precursor gases (red), and with photolysis and precursor gases (purple).

In the case where these is only one molecular absorber, Equations 2.3 and 2.6 can be combined to determine α

$$\alpha = \frac{1}{c}\left(\frac{1}{\tau_1} - \frac{1}{\tau_2}\right) \qquad \text{(Equation 2.7)}$$

where τ_1 is the ringdown time with the molecular absorber, and τ_2 is the ringdown time of the empty cavity. In the case where precursor gases are photolyzed, as in the experiments

in this work, Equation 2.7 can be altered to take into account the absorbance due to the photolytic species and their resulting chemistry, as seen in Figure 2.1

$$\alpha = \frac{1}{c}\left(\frac{1}{\tau_{Photolysis\ on}} - \frac{1}{\tau_{Photolysis\ off}}\right) \qquad \text{(Equation 2.8)}$$

Since its inception, CRDS has gained widespread usage due to its sensitivity, using both pulsed and continuous sources. Many of its applications have been for studying molecules with low concentrations, such as reactive radicals, molecular clusters, or isotopologues, where the high sensitivity is required.[4] Weak transitions, such as overtones or forbidden transitions have also been extensively studied with CRDS.[2] With the development of time-dependent methods of spectral analysis, it has been used to measure reaction rate constants,[5] and for fast reactions, the Simultaneous Kinetics and Ringdown (SKaR) method has been developed.[6] Its range of application extends as far as usage in atmospheric field campaigns,[7-8] and for medical diagnostics of human breath.[9]

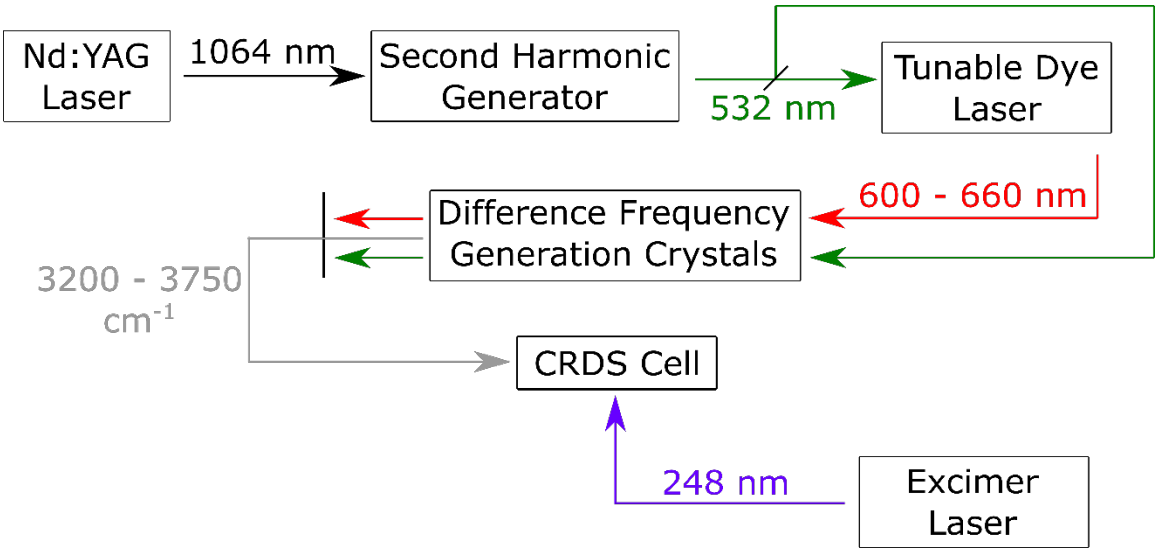

Figure 2.2: The pulsed laser photolysis, mid-infrared cavity ringdown spectrometer used in these experiments.

A schematic of the CRDS instrument used in this work can be seen in Figure 2.2. The pulsed laser used here provides a wider tunability than available in continuous lasers,

at the cost of broader linewidths (estimated to be ~1 cm^{-1} in the mid-infrared design used here.) This instrument operates in the mid-infrared (3200 – 3750 cm^{-1}) to look at the OH-stretches of molecules. The second harmonic (532 nm) of a 10 Hz Nd:YAG laser (Continuum Surelite III) is passed through a 30/70 beam splitter. 30% of the 532 nm light is sent through a tunable dye laser (Quanta Ray PDL-3) containing DCM (4-(dicyanomethylene)-2-methyl-6-(4-dimethylaminostyryl)-4H-pyran, Exciton) dye in a methanol solution, producing light in the 600 – 660 nm range. This output is recombined with the remaining 70% of the 532 nm light. This then goes through two KTP (potassium titanyl phosphate) crystals, where a mid-IR photon is produced through difference frequency generation[10] and therefore has a frequency equal to that of the difference of the two pump beams. Filters block the remaining green and red beams and the mid-IR beam is sent into the CRDS cell containing ringdown mirrors with R = 0.9998 (2.8 μm, Los Gatos Research); the mirror reflectivity of these mirrors over the mid-infrared range can be seen in Figure 2.3. Perpendicularly to the CRDS axis, a KrF excimer laser (Lambda Physik LPX 210i), also operating at 10 Hz, fires at 248 nm to initiate the chemistry through pulsed laser photolysis. The resulting signal, collected for 80-100 microseconds at 25 MHz, is detected by a liquid nitrogen cooled InSb detector (Infrared Associates Inc., IS-0.50) and digitized with an analog-to-digital converter (Gage). Custom written LabView is used to collect and average 16 ringdowns, which are subsequently fit using a Levenberg-Marquadt algorithm.

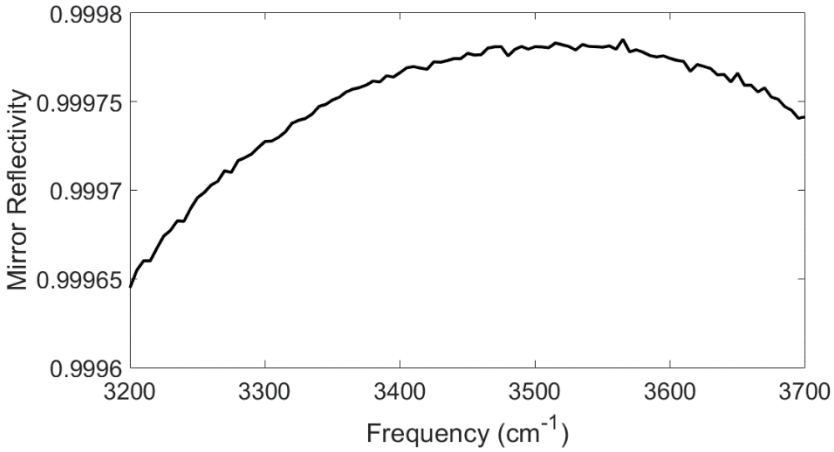

Figure 2.3: The reflectivity of the mid-infrared CRDS mirrors centered at 2.8 μm used in experiments.

2.1b – Laser-Induced Fluorescence

Laser-induced fluorescence, first developed in 1968,[11] is a method in which first, a specific transition is excited. The excited state that emits a photon through spontaneous emission (fluorescence) within a time frame of nanoseconds to microseconds, depending on the transition and conditions of the excited molecule. The emitted photon can either be at the same wavelength as the initial excitation laser, in a process known as 'on-resonance fluorescence', or at a different wavelength to end up in a different state than the initial state, known as 'off-resonance fluorescence'. Many experiments use a narrowband filter to prevent fluorescence at multiple wavelengths from being detected by the photomultiplier tube detector. An example of an off-resonance detection scheme, used to detect OH (v = 0), can be seen in Figure 2.4.

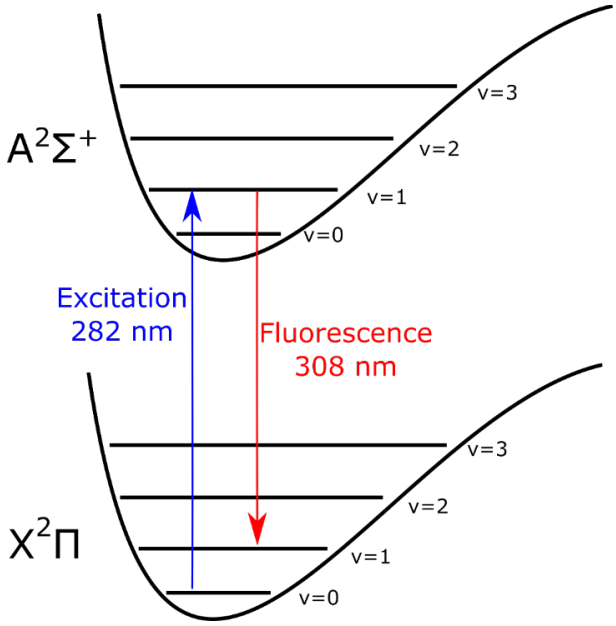

Figure 2.4: The LIF excitation and detection scheme for detecting OH (v = 0) with the $A^2\Sigma^+$ - $X^2\Pi$ electronic transition.

LIF is a highly sensitive technique and has been used to detect concentrations as low as 10^6 cm^{-3}.[12] It is commonly used in pulsed laser photolysis gas phase kinetics measurements, by varying the time delay between the photolysis laser and the LIF excitation laser, which is used to detect a reactive radical, such as OH or CN, under pseudo-first order conditions.

Two LIF excitation schemes are used in this work to detect the CN and OH (v = 0, 1) radicals. To detect the CN radical, the 355 nm third harmonic of a Nd:YAG laser (Continuum Powerlite Precision II) firing at 10 Hz is put into a dye laser (Laser Analytical Systems, , LDL 20505) containing Exalite 389 dye (Exciton) in 1,4-dioxane (Sigma Aldirch, 99.8%), to produce light at ~389 nm to excite the CN $B^2\Sigma^+$ - $X^2\Sigma^+$ (0,0) transition. Fluorescence is then detected from the (0,1) transition at ~420 nm. An excimer laser (Coherent LPXPro 210), also operating at 10 Hz, is used to initiate the radical chemistry.

Fluorescence was detected from the CN (0,1) transition at ~420 nm by a photomultiplier tube (Thorn EMI 6723) preceded by a 420 nm bandpass filter (Ealing Optics).

To detect the OH radical, the 532 nm second harmonic of a 10 Hz Nd:YAG (Continuum Powerlite Precision II) laser is used to excite a dye laser containing either Rhodamine 6G (Exciton), for OH $\nu = 0$, or a mix of Rhodamine 6G and Rhodamine B (Exicton), for $\nu = 1$, the output of which is sent through BBO doubling crystals to produce ~1 mJ of UV light to excite the OH radicals. The (1,0) and (2,1) bands of the $A^2\Sigma^+ \leftarrow X^2\Pi$ electronic transition are used to excite the OH ($\nu = 0$) and OH ($\nu = 1$) radicals, respectively, at ~282 and ~289 nm. The resulting fluorescence is detected by a photomultiplier tube proceeded by either a 310 (for OH $\nu = 0$) or 320 nm (for OH $\nu = 1$) bandpass filter. An excimer laser (Lambda Physics COMPexPro 201) operating at either 193 or 248 nm at 10 Hz is used to create the radicals of interest.

2.2 – Flow Cells

In order to study the temperature-dependence of reactions, different methods may be used depending on the desired temperature range. Here, we use a temperature-controlled flow cell for studying atmospheric chemistry experiments over the range of 253 – 333 K and 50 – 700 torr. Experiments studying astrochemical reactions use the CRESU (*Cinétique de Réaction en Ecoulement Supersonique Uniforme*; a French acronym for 'reaction kinetics in a uniform supersonic flow'), which allows for a cold flow in thermal equilibrium to temperatures as cold as a few K.

2.2a – Temperature-Controlled Flow Cell

To measure the temperature-dependent branching ratios of the OH + NO_2 reaction, a custom-designed temperature-controlled flow cell, as seen in Figure 2.5 was developed

by Luis Gomez and used in this work. This flow cell uses thermoelectric coolers (TECs, TE Technologies TE-63-1.4-1.15), controlled by a temperature controller (ILX Lightwave LDT-5948) to cool or heat the cell between 253 and 333 K, as measured by a resistance temperature detector (RTD) attached to the cell. A circulator filled with water, methanol, or a mixture of the two, helps stabilize the temperature throughout the cell and reduce any temperature gradients. Before entering the cell, gas flows through a stainless-steel pre-cooling block that is also in thermal contact with the bottom of the cell.

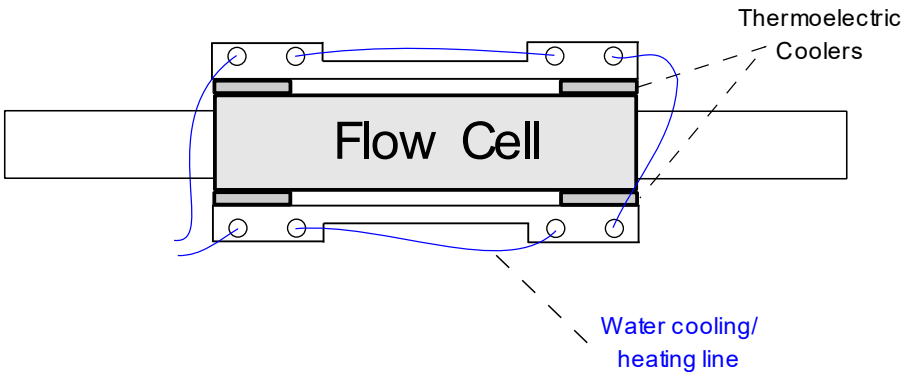

Figure 2.5: Top view of the temperature-controlled flow cell used in CRDS experiments in this work. TECs are placed on each corner of the cell. To stabilize the temperature, circulated water, methanol or mixtures thereof are in thermal contact with the cell.

2.2b – CRESU

In order to study bimolecular or termolecular reaction kinetics, the gases must be in thermal equilibrium. However, achieving this is difficult at the very cold temperatures relevant to astrochemistry (~10 K). Liquid N_2 has a temperature of 77 K,[13] and therefore cannot cool gas flows below that. Furthermore, even at 77 K and above, the wall-cooling method means that at these cold temperatures, many species with lower vapor pressures will stick to the wall upon collision. This further limits the number of reactions that can be studied through liquid N_2 cooling. One of the most common techniques for cooling molecules to < 10 K is the supersonic free jet expansion, where molecules are expanded

through a narrow nozzle into a low-pressure chamber. While extensively used in spectroscopy to measure cold spectra of unstable species, the low number of collisions means the system does not reach thermal equilibrium and in fact has large temperature and pressure gradients.[14] In recent years, helium buffer gas cooling has been developed to effectively cool molecules to < 10 K,[15] but has not yet been applied to *in situ* studies of bimolecular reactions. Ultracold (500 nK) chemical reactions have been directly observed after laser cooling the reactants,[16] but the number of compounds that can be cooled to these temperatures is extremely limited.

The CRESU technique was developed in the 1980s[17] for studying astrochemical reactions and energy transfer processes and has been the subject of previous reviews[18-20]. While initially used in conjunction with a mass spectrometer to measure the rate constants of ion-neutral reactions, it has since been combined with a wide range of sensitive detection methods. CRESU flows have been used to reach temperatures as low as 6 K.[21]

Briefly, the core of the CRESU technique is the Laval nozzle (also known as a de Laval nozzle), which are specially designed convergence-divergence nozzles. Laval nozzles were originally developed in the late 19th century and have been used extensively in mechanical engineering, including in the propulsion of rockets. As can be seen in Figure 2.6A, in CRESU experiments, gas is pumped from a high pressure reservoir, typically but not always held at room temperature, through a Laval nozzle, before being isentropically expanded into a low pressure chamber at supersonic speeds. As the gas is compressed and expanded through the nozzle, it is cooled, allowing the cold temperatures necessary for astrochemical experiments to be reached. Surrounding the cold, uniform flow (known as the core), boundary layers with varying temperatures and pressures are also formed. A key

advantage of the CRESU method is that it does not require collisions with a wall to cool the molecules and is functionally wall-less.[19] This allows for molecules with low vapor pressures to be studied at these cold temperatures.

The temperature of a CRESU flow, T_{flow}, can be calculated with

$$T_{flow} = T_0 \left(1 + \frac{\gamma-1}{2} M^2\right)^{-1} \quad \text{(Equation 2.9)}$$

where T_0 is the temperature of the reservoir, γ is the ratio of the specific heat capacities C_p/C_v of the buffer gas (typically N_2, He or Ar), and M is the Mach number of the expansion. This value is experimentally measured to characterize the nozzle before use in chemical kinetics measurements, as described below.

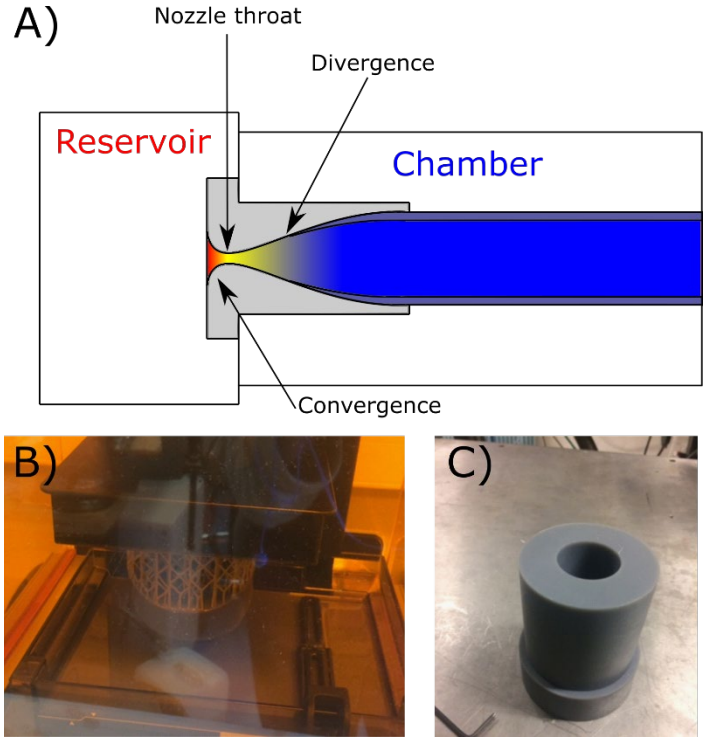

Figure 2.6: (A): A diagram of a Laval nozzle, showing gas being compressed in the convergent portion of the nozzle, before reaching the minimum diameter at the throat and being expanded through the divergent portion of the nozzle to produce a cold uniform flow. (B): A Laval nozzle being 3D printed. (C): Example of a Laval nozzle.

The temperature and density of the cold uniform flow is a function of the nozzle's geometry, and they must be carefully designed to create suitable nozzles. The advent of high precision 3D printers has allowed for faster manufacturing of Laval nozzles, as can be seen in Figure 2.6B and 2.6C. Due to imperfections in the manufacturing, however, all nozzles must be tested prior to use in experiments to characterize the flow and determine the necessary conditions for achieving a stable flow.

The method for testing the nozzle uses a Pitot probe to conduct impact pressure measurements. This probe is a hollow tube inserted into the flow; impact of the supersonic flow with the Pitot probe creates a shockwave. The impact pressure from this shockwave is measured by a pressure sensor attached to the Pitot tube. The pressure measured by the Pitot can then be related to the reservoir pressure with

$$P_i = P_r \left(\frac{(\gamma+1)M^2}{(\gamma-1)M^2+2}\right)^{\frac{\gamma}{\gamma-1}} \left(\frac{\gamma+1}{2\gamma M^2-\gamma+1}\right)^{\frac{1}{\gamma-1}} \quad \text{(Equation 2.10)}$$

Which allows for the Mach number M to be determined. From that, the temperature can then be determined using Equation 2.9. By varying the position of the Pitot tube throughout the supersonic flow, the width and length of the uniform core can be determined. An example of Pitot measurements can be seen in Figure 2.7.

The typical densities of these uniform supersonic flows are 10^{16} – 10^{17} cm^{-3}.[19] Concentrations of the reactants and precursors must be kept under < 1% of the total flow rate to not disturb the uniformity of the flow. At concentrations higher than this, the uniformity of the flow is destroyed, making it unable to be used in spectroscopy and kinetics experiments. This imposes an upper limit on the rate constants that can be measured with CRESU to roughly ≥ 10^{-12} cm^3 s^{-1}.[19] However, if the reactant is also the buffer gas, then faster rates can be measured. This was done in Tizniti et al.,[22] who

measured the rate constant of the F + H_2 reaction down to 11 K, where its rate is 2.48 × 10^{-13} cm^3 s^{-1}, by using a buffer gas of pure H_2 at the lowest temperatures.

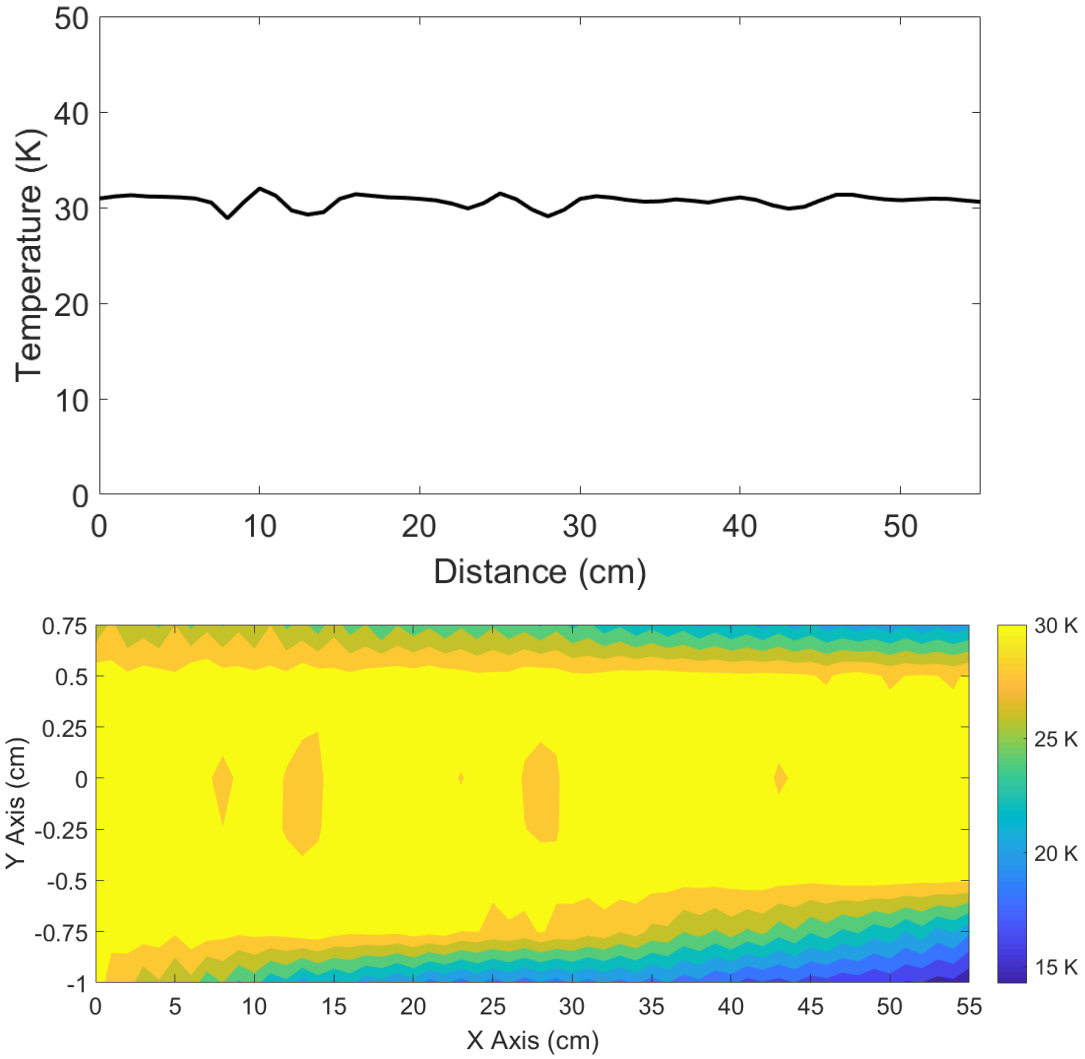

Figure 2.7: One-dimensional (top), along the y = 0 cm position, and two-dimensional (bottom) Pitot probe impact measurements of a 30 K N_2 Laval nozzle. Note that outside of the core, the flow is not isentropic with the reservoir and thus the temperature is not accurately calculated with Equations 2.9 and 2.10.

The gas flows used in CRESU experiments can be continuous or pulsed; pulsed CRESU instruments can be pulsed between the gas inlet and the reservoir, or between the reservoir and the chamber. Continuous CRESU flows require extremely powerful pumps in order to pump the gas at the necessary supersonic speeds in the chamber. Pulsed CRESU

has historically pulsed between the gas inlet and the reservoir, which is unable to reach as low temperatures as continuous flows due to a smaller pressure differential between the reservoir and chamber. In recent years, a new method of pulsed CRESU, which uses a rapidly rotating aerodynamic chopper between the reservoir and the chamber, has been developed and allows pulsed CRESU to reach lower temperatures, but is technically demanding.[23]

In the experiments presented in this thesis, CRESU flows are used in conjunction with PLP-LIF in order to measure bimolecular rate constants down to 15 K in experiments done in collaboration with the University of Rennes 1. Figure 2.8 shows a schematic of the instrument used in this work. The LIF excitation beam passes into the CRESU flow through the nozzle. The LIF emission is then detected by a photomultiplier tube (PMT) placed above the supersonic flow, with an appropriate filter to exclude other wavelengths. To initiate the radical chemistry, an excimer laser fires through the CRESU flow; the timing between the excimer and the Nd:YAG lasers is controlled by a delay generator.

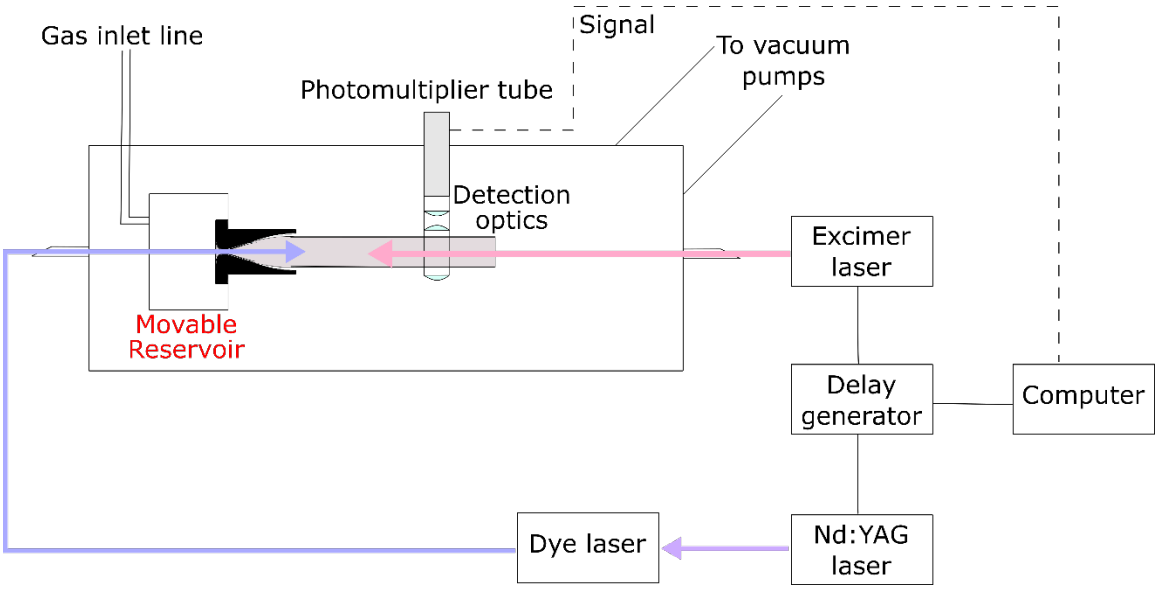

Figure 2.8: The CRESU PLP-LIF instrument used to measure bimolecular reaction rate constants in this work.

2.3 – References

1. Anderson, D. Z.; Frisch, J. C.; Masser, C. S., Mirror Reflectometer Based on Optical Cavity Decay Time. *Appl Optics* **1984**, *23*, 1238-1245.

2. O'Keefe, A.; Deacon, D. A. G., Cavity Ring-Down Optical Spectrometer for Absorption-Measurements Using Pulsed Laser Sources. *Rev Sci Instrum* **1988**, *59*, 2544-2551.

3. Busch, K. W.; Busch, M. A., *Cavity-Ringdown Spectroscopy : An Ultratrace-Absorption Measurement Technique*; American Chemical Society ; Distributed by Oxford University Press: Washington, DC New York, 1999, p xii, 269 p.

4. Scherer, J. J.; Paul, J. B.; O'Keefe, A.; Saykally, R. J., Cavity Ringdown Laser Absorption Spectroscopy: History, Development, and Application to Pulsed Molecular Beams. *Chem Rev* **1997**, *97*, 25-51.

5. Yu, T.; Lin, M. C., Kinetics of Phenyl Radical Reactions Studied by the Cavity-Ring-Down Method. *J Am Chem Soc* **1993**, *115*, 4371-4372.

6. Brown, S. S.; Ravishankara, A. R.; Stark, H., Simultaneous Kinetics and Ring-Down: Rate Coefficients from Single Cavity Loss Temporal Profiles. *J Phys Chem A* **2000**, *104*, 7044-7052.

7. Richardson, S. J.; Miles, N. L.; Davis, K. J.; Crosson, E. R.; Rella, C. W.; Andrews, A. E., Field Testing of Cavity Ring-Down Spectroscopy Analyzers Measuring Carbon Dioxide and Water Vapor. *J Atmos Ocean Tech* **2012**, *29*, 397-406.

8. Bitter, M.; Ball, S. M.; Povey, I. M.; Jones, R. L., A Broadband Cavity Ringdown Spectrometer for in-situ Measurements of Atmospheric Trace Gases. *Atmos Chem Phys* **2005**, *5*, 2547-2560.

9. Sun, M. X.; Jiang, C. Y.; Gong, Z. Y.; Zhao, X. M.; Chen, Z. Y.; Wang, Z. N.; Kang, M. L.; Li, Y. X.; Wang, C. J., A Fully Integrated Standalone Portable Cavity Ringdown Breath Acetone Analyzer. *Rev Sci Instrum* **2015**, *86*.

10. Reid, S. A.; Tang, Y., Generation of Tunable, Narrow-Band Mid-Infrared Radiation through a 532 nm Pumped KTP Optical Parametric Amplifier. *Appl Optics* **1996**, *35*, 1473-1477.

11. Tango, W. J.; Link, J. K.; Zare, R. N., Spectroscopy of K_2 Using Laser-Induced Fluorescence. *J Chem Phys* **1968**, *49*, 4264-&.

12. Heard, D. E.; Pilling, M. J., Measurement of OH and HO_2 in the Troposphere. *Chem Rev* **2003**, *103*, 5163-5198.

13. Jacobsen, R. T.; Stewart, R. B.; Jahangiri, M., Thermodynamic Properties of Nitrogen from the Freezing Line to 2000 K at Pressures to 1000 MPa. *J Phys Chem Ref Data* **1986**, *15*, 735-909.

14. Smalley, R. E.; Wharton, L.; Levy, D. H., Molecular Optical Spectroscopy with Supersonic Beams and Jets. *Accounts Chem Res* **1977**, *10*, 139-145.

15. Hutzler, N. R.; Lu, H. I.; Doyle, J. M., The Buffer Gas Beam: An Intense, Cold, and Slow Source for Atoms and Molecules. *Chem Rev* **2012**, *112*, 4803-4827.

16. Hu, M. G.; Liu, Y.; Grimes, D. D.; Lin, Y. W.; Gheorghe, A. H.; Vexiau, R.; Bouloufa-Maafa, N.; Dulieu, O.; Rosenband, T.; Ni, K. K., Direct Observation of Bimolecular Reactions of Ultracold KRb Molecules. *Science* **2019**, *366*, 1111-+.

17. Rowe, B. R.; Dupeyrat, G.; Marquette, J. B.; Gaucherel, P., Study of the Reactions $N_2^+ + 2\ N_2 \rightarrow N_4^+ + N_2$ and $O_2^+ + 2\ O_2 \rightarrow O_4^+ + O_2$ from 20 to 160 K by the CRESU Technique. *J Chem Phys* **1984**, *80*, 4915-4921.

18. Sims, I. R.; Queffelec, J. L.; Defrance, A.; Rebrionrowe, C.; Travers, D.; Bocherel, P.; Rowe, B. R.; Smith, I. W. M., Ultralow Temperature Kinetics of Neutral-Neutral Reactions - the Technique and Results for the Reactions $CN+O_2$ Down to 13 K and $CN+NH_3$ Down to 25 K. *J Chem Phys* **1994**, *100*, 4229-4241.

19. Fournier, M.; Le Picard, S. D.; Sims, I. R., Chapter 1: Low-Temperature Chemistry in Uniform Supersonic Flows. In *Cold Chemistry: Molecular Scattering and Reactivity near Absolute Zero*, The Royal Society of Chemistry: 2018; pp 1-45.

20. Cooke, I. R.; Sims, I. R., Experimental Studies of Gas-Phase Reactivity in Relation to Complex Organic Molecules in Star-Forming Regions. *ACS Earth Space Chem* **2019**, *3*, 1109-1134.

21. Lara, M.; Berteloite, C.; Paniagua, M.; Dayou, F.; Picard, S. D.; Launay, J. M., Experimental and Theoretical Study of the Collisional Quenching of $S(^1D)$ by Ar. *Phys Chem Chem Phys* **2017**, *19*, 28555-28571.

22. Tizniti, M.; Le Picard, S. D.; Lique, F.; Berteloite, C.; Canosa, A.; Alexander, M. H.; Sims, I. R., The Rate of the $F + H_2$ Reaction at Very Low Temperatures. *Nat Chem* **2014**, *6*, 141-145.

23. Jimenez, E.; Ballesteros, B.; Canosa, A.; Townsend, T. M.; Maigler, F. J.; Napal, V.; Rowe, B. R.; Albaladejo, J., Development of a Pulsed Uniform Supersonic Gas Expansion System Based on an Aerodynamic Chopper for Gas Phase Reaction Kinetic Studies at Ultra-Low Temperatures. *Rev Sci Instrum* **2015**, *86*.